

Ghost-gluon coupling, power corrections and $\Lambda_{\overline{MS}}$ from twisted-mass lattice QCD at $N_f=2$

B. Blossier^a, Ph. Boucaud^a, F. De soto^b, V. Morenas^c
M. Gravina^a, O. Pène^a, J. Rodríguez-Quintero^d



^aLaboratoire de Physique Théorique¹

CNRS et Université Paris-Sud XI, Bâtiment 210, 91405 Orsay Cedex, France

^b Dpto. Sistemas Físicos, Químicos y Naturales,
Universidad Pablo de Olavide, 41013 Sevilla, Spain.

^c Laboratoire de Physique Corpusculaire, Université Blaise Pascal, CNRS/IN2P3
63000 Aubière Cedex, France.

^d Dpto. Física Aplicada, Fac. Ciencias Experimentales,
Universidad de Huelva, 21071 Huelva, Spain.

Abstract

We present results concerning the non-perturbative evaluation of the ghost-gluon running QCD coupling constant from $N_f = 2$ twisted-mass lattice calculations. A novel method for calibrating the lattice spacing, independent of the string tension and hadron spectrum is presented with results in agreement with previous estimates. The value of $\Lambda_{\overline{MS}}$ is computed from the running of the QCD coupling only after extrapolating to zero dynamical quark mass and after removing a non-perturbative OPE contribution that is assumed to be dominated by the dimension-two $\langle A^2 \rangle$ gluon condensate. The effect due to the dynamical quark mass in the determination of $\Lambda_{\overline{MS}}$ is discussed.

LPT-Orsay 10-37

UHU-FT/10-31

¹Unité Mixte de Recherche 8627 du Centre National de la Recherche Scientifique

Contents

1	Introduction	2
2	The running coupling in Taylor scheme	4
2.1	Pure perturbation theory	5
2.2	OPE power corrections	7
3	The lattice computation of the Taylor coupling	9
3.1	The lattice action	9
3.2	The computation of the gluon and ghost Green functions	10
3.3	On the treatment of lattice artefacts	11
3.3.1	Hypercubic $H(4)$ -extrapolation	12
3.3.2	Quark mass artefacts	13
4	Computing $\Lambda_{\overline{\text{MS}}}$ and the gluon condensate	17
4.1	Looking for the “plateau”	17
4.2	Global fit and the calibration of lattice spacing	18
4.3	The contribution from the Wilson coefficient higher orders	19
4.4	Discussing the systematical uncertainties	20
4.4.1	Volume effects	21
4.4.2	Three-loop versus four-loop confrontation	21
4.4.3	The impact of higher-orders in the OPE expansion	21
4.5	Conversion to physical units and quark mass effect	22
5	Discussions and conclusions	25
A	Appendix: The Wilson coefficients at the four-loops order	28

1 Introduction

QCD is believed to be the theory of the strong interactions with, as only inputs, one mass parameter for each quark species and the value of the QCD coupling constant at some energy or momentum scale in some renormalization scheme (Alternatively, this last free parameter of the theory can be fixed by Λ_{QCD} , the energy scale used as the typical boundary condition for the integration of the Renormalization Group equation for the strong coupling constant). This is the parameter which expresses the scale of strong interactions, the only parameter in the limit of massless quarks. While the evolution of the coupling with the momentum scale is determined by the quantum corrections induced by the renormalization of the bare coupling and can be computed in perturbation theory, the strength itself of the interaction, given at any scale by the value of

the renormalized coupling at this scale, or equivalently by Λ_{QCD} , is one of the above mentioned parameters of the theory and has to be taken from experiment.

The QCD running coupling can be also obtained from lattice computations, the free parameters being adjusted from experimental numbers, masses, decay constants etc. These parameters being settled, the lattice calculation of Λ_{QCD} proceeds in several manners: the implementation of the Schrödinger functional scheme (see, for instance, [1–4] and references therein), those based on the perturbative analysis of short-distance sensitive lattice observables as the “boosted” lattice coupling (see for instance [5–8] and reference therein) and, in particular, those based on the study of the momentum behaviour of Green functions (see [9–16] and references therein) are among the most extendedly applied. Indeed, the confrontation of the behaviour with respect to the renormalization scale of 2-gluon and 3-gluon Green functions with the corresponding perturbative predictions leaves us with a good estimate of α_S , its running leading to the determination of Λ_{QCD} , but also reveals a dimension-two non-zero gluon condensate in the Landau gauge. The possible phenomenological implications in the gauge-invariant world of such a dimension-two gluon condensate and in connection with confinement scenarios has been also largely investigated (see for instance [17]).

In [18], the Green’s function approach proposed in ref. [16] was followed exploiting a non-perturbative definition of the coupling derived from the ghost and gluon propagators for the determination of $\Lambda_{\overline{\text{MS}}}$ in pure Yang-Mills ($N_f = 0$). In that work, the renormalization scheme for the ghost-gluon vertex corresponding to the latter coupling was properly defined. The *quenched* lattice results were analyzed over a wide momentum window, applying a “plateau” procedure to extract simultaneously both $\Lambda_{\overline{\text{MS}}}$ and the gluon condensate. The result is consistent with other calculations, for the description of the gluon and ghost Green functions and for the running of the strong coupling in “*quenched*” QCD.

In the present paper we extend [18] to the case in which twisted $N_f = 2$ dynamical quarks are included in the lattice simulations for several different bare lattice couplings ($\beta = 3.9, 4.05, 4.2$) and different dynamical quark masses. We use the configurations produced by the ETM Collaboration [19]. This offers the opportunity to study the effect of the quark mass on the lattice determination of the strong coupling, and we will see that this effect is far from negligible. Similar works have started some time ago [15] using *unquenched* lattice configurations with, at first, rather heavy $N_f = 2$ dynamical quarks, and continuing more recently [3, 16] in a more realistic case. The comparison of our current results with those needs certainly due account of the dependence on the dynamical masses.

Let us now summarize our strategy. For every value μ of the momentum scale we compute, from the lattice simulations, the value of the strong coupling constant. This can be converted via a four loops formula to a value for $\Lambda_{\overline{\text{MS}}}(\mu)$. $\Lambda_{\overline{\text{MS}}}$ is a scale independent constant which sets the strong interaction scale. It results that $\Lambda_{\overline{\text{MS}}}(\mu)$ should be independent of μ as soon as we are in the perturbative regime. As we shall see, this is far from true at energies of several GeV’s, which are generally believed to lie in the perturbative regime. This surprising feature was already noticed in the quenched case [18]. We then need to take into account non-perturbative contributions using

Wilson expansion. In Landau gauge there exists only one dimension two operator : $A^2 \equiv A_a^\mu A_\mu^a$. The Wilson coefficient of that operator has been computed to order α^4 [20]. We will assume that only this A^2 operator contributes ². We fit $\langle A^2 \rangle$ so that, once the non-perturbative contribution subtracted, one gets a good “plateau” for $\Lambda_{\overline{\text{MS}}}(\mu)$. We thus get an estimate of both $\Lambda_{\overline{\text{MS}}}$ and $\langle A^2 \rangle$.

The paper is organized as follows. In section 2, we outline and discuss all the analytical tools, perturbation theory and Wilson expansion, needed to describe the running coupling in the appropriate renormalization scheme. In section 3, we give the details of the lattice computation of the coupling, describe the treatment of lattice artefacts and depict the analysis procedure leading to the estimate of $\Lambda_{\overline{\text{MS}}}$ and the gluon condensate. The analysis is performed in section 4, where we also present the results and discuss different sources of systematical uncertainties (special attention is paid to the higher order contribution in both the perturbative and the OPE expansions). Finally, we conclude in section 5.

2 The running coupling in Taylor scheme

Among the many possibilities to compute a strong coupling α_S from lattice simulations, it has been shown [18] that the so-called Taylor scheme is among the most tractable ones because, with the help of the so-called Non-renormalization Taylor theorem, the coupling can be computed from two-point Green functions renormalized in MOM scheme. Following the usual notation we will write Landau gauge gluon and ghost propagators as:

$$\begin{aligned} (G^{(2)})_{\mu\nu}^{ab}(p^2, \Lambda) &= \frac{G(p^2, \Lambda)}{p^2} \delta_{ab} \left(\delta_{\mu\nu} - \frac{p_\mu p_\nu}{p^2} \right), \\ (F^{(2)})^{a,b}(p^2, \Lambda) &= -\delta_{ab} \frac{F(p^2, \Lambda)}{p^2}; \end{aligned} \quad (2.1)$$

with Λ the regularisation cutoff ($a^{-1}(\beta)$ if, for instance, we specialise to lattice regularisation). The renormalized dressing functions, G_R and F_R are defined through :

$$\begin{aligned} G_R(p^2, \mu^2) &= \lim_{\Lambda \rightarrow \infty} Z_3^{-1}(\mu^2, \Lambda) G(p^2, \Lambda) \\ F_R(p^2, \mu^2) &= \lim_{\Lambda \rightarrow \infty} \tilde{Z}_3^{-1}(\mu^2, \Lambda) F(p^2, \Lambda), \end{aligned} \quad (2.2)$$

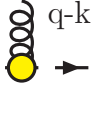
with standard MOM renormalization condition

$$G_R(\mu^2, \mu^2) = F_R(\mu^2, \mu^2) = 1. \quad (2.3)$$

Then, we can consider the ghost-gluon vertex which could be non-perturbatively obtained through a three-point Green function, defined by two ghost and one gluon fields, with amputated legs after

² It is indeed not easy with present accuracy to discard higher order operators.

dividing by two ghost and one gluon propagators. This vertex can be written quite generally as:

$$\tilde{\Gamma}_\nu^{abc}(-q, k; q-k) = \frac{-}{k} \rightarrow \text{diagram} \rightarrow \frac{-}{q} = i g_0 f^{abc} (q_\nu H_1(q, k) + (q-k)_\nu H_2(q, k)) , \quad (2.4)$$


where $H_{1,2}$ are the two involved independent scalar form factors, g_0 is the bare strong coupling, q is the outgoing ghost momentum and k the incoming one. This bare three-point Green function will be renormalized according to:

$$\tilde{\Gamma}_R = \tilde{Z}_1 \Gamma. \quad (2.5)$$

In the MOM renormalization procedure, as explained in ref. [18], \tilde{Z}_1 is fully determined by demanding that one specific combination of those two form factors (chosen at one's will) be equal to its tree-level value for a specific kinematical configuration; while

$$g_R(\mu^2) = \lim_{\Lambda \rightarrow \infty} Z_g^{-1}(\mu^2, \Lambda^2) g_0(\Lambda^2) = \lim_{\Lambda \rightarrow \infty} \frac{Z_3^{1/2}(\mu^2, \Lambda^2) \tilde{Z}_3(\mu^2, \Lambda^2)}{\tilde{Z}_1(\mu^2, \Lambda^2)} g_0(\Lambda^2) , \quad (2.6)$$

where one puts explicitly the cut-off dependence. If one turns now to the Taylor scheme, *i.e.* a specific MOM-type renormalization scheme defined by a kinematical configuration with **zero incoming ghost momentum**, one obtains [21]

$$\tilde{Z}_1(\mu^2, \Lambda^2) \equiv 1 ; \quad (2.7)$$

and one is left with

$$\alpha_T(\mu^2) \equiv \frac{g_T^2(\mu^2)}{4\pi} = \lim_{\Lambda \rightarrow \infty} \frac{g_0^2(\Lambda^2)}{4\pi} G(\mu^2, \Lambda^2) F^2(\mu^2, \Lambda^2) ; \quad (2.8)$$

where we also apply the renormalization condition for the propagators, eqs. (2.2,2.3), to replace the renormalization constants, Z_3 and \tilde{Z}_3 , by the bare dressing functions. As emphasized in [18], the remarkable feature of eq. (2.8) is that it involves only F and G so that no measure of the ghost-gluon vertex is needed for the determination of the coupling constant.

2.1 Pure perturbation theory

The Taylor coupling and the one renormalized in the standard $\overline{\text{MS}}$ prescription, as any other different definitions of the coupling constant, can be related through:

$$\alpha_T(\mu^2) = \bar{\alpha}(\mu^2) \left(1 + \sum_{i=1} c_i \left(\frac{\bar{\alpha}(\mu^2)}{4\pi} \right)^i \right) ; \quad (2.9)$$

where the coefficients c_i 's can be obtained in perturbation theory [22, 23]

$$\begin{aligned}
c_1 &= \frac{507 - 40N_f}{36}, \\
c_2 &= \frac{76063}{144} - \frac{351}{8}\zeta(3) - \left(\frac{1913}{27} + \frac{4}{3}\zeta(3)\right) N_f + \frac{100}{91}N_f^2 \\
c_3 &= \frac{42074947}{1728} - \frac{60675}{16}\zeta(3) - \frac{70245}{64}\zeta(5) - \left(\frac{769387}{162} - \frac{8362}{27}\zeta(3) - \frac{2320}{9}\zeta(5)\right) N_f \\
&\quad + \left(\frac{199903}{972} + \frac{28}{9}\zeta(3)\right) N_f^2 - \frac{1000}{729} N_f^3.
\end{aligned} \tag{2.10}$$

It was proven in ref. [18] that these coefficients could be also directly derived from the anomalous dimensions for gluon and ghost propagators, as eq. (2.8) indicates. The three coefficients in eq. (2.10) obviously define unambiguously the running of α_T up to four-loops given by

$$\begin{aligned}
\alpha_T(\mu^2) &= \frac{4\pi}{\beta_0 t} \left(1 - \frac{\beta_1 \log(t)}{\beta_0^2 t} + \frac{\beta_1^2}{\beta_0^4 t^2} \left(\left(\log(t) - \frac{1}{2} \right)^2 + \frac{\tilde{\beta}_2 \beta_0}{\beta_1^2} - \frac{5}{4} \right) \right) \\
&\quad + \frac{1}{(\beta_0 t)^4} \left(\frac{\tilde{\beta}_3}{2\beta_0} + \frac{1}{2} \left(\frac{\beta_1}{\beta_0} \right)^3 \left(-2 \log^3(t) + 5 \log^2(t) + \left(4 - 6 \frac{\tilde{\beta}_2 \beta_0}{\beta_1^2} \right) \log(t) - 1 \right) \right)
\end{aligned} \tag{2.11}$$

with $t = \ln \frac{\mu^2}{\Lambda_T^2}$, since the coefficients of the β -function of α_T ,

$$\beta_T(\alpha_T) = \frac{d\alpha_T}{d \ln \mu^2} = -4\pi \sum_{i=0} \tilde{\beta}_i \left(\frac{\alpha_T}{4\pi} \right)^{i+2}, \tag{2.12}$$

can be derived,

$$\begin{aligned}
\tilde{\beta}_0 &= \bar{\beta}_0 = 11 - \frac{2}{3}N_f \\
\tilde{\beta}_1 &= \bar{\beta}_1 = 102 - \frac{38}{3}N_f \\
\tilde{\beta}_2 &= \bar{\beta}_2 - \bar{\beta}_1 c_1 + \bar{\beta}_0 (c_2 - c_1^2) \\
&= 3040.48 - 625.387 N_f + 19.3833 N_f^2 \\
\tilde{\beta}_3 &= \bar{\beta}_3 - 2\bar{\beta}_2 c_1 + \bar{\beta}_1 c_1^2 + \bar{\beta}_0 (2 c_3 - 6 c_2 c_1 + 4 c_1^3) \\
&= 100541 - 24423.3 N_f + 1625.4 N_f^2 - 27.493 N_f^3,
\end{aligned} \tag{2.13}$$

from the knowledge of those coefficients, c_i 's, and from that of the standard $\overline{\text{MS}}$ β -function,

$$\beta_{\overline{\text{MS}}}(\bar{\alpha}) = \frac{d\bar{\alpha}}{d \ln \mu^2} = -4\pi \sum_{i=0} \bar{\beta}_i \left(\frac{\bar{\alpha}}{4\pi} \right)^{i+2} \tag{2.14}$$

definition (details of the computation can be found in [13, 18, 26]), one gets at tree level

$$\begin{aligned} F_R(q^2, \mu^2) &= F_{R,\text{pert}}(q^2, \mu^2) \left(1 + \frac{3}{q^2} \frac{g_R^2 \langle A^2 \rangle_{R, \mu^2}}{4(N_C^2 - 1)} \right) \\ G_R(q^2, \mu^2) &= G_{R,\text{pert}}(q^2, \mu^2) \left(1 + \frac{3}{q^2} \frac{g_R^2 \langle A^2 \rangle_{R, \mu^2}}{4(N_C^2 - 1)} \right), \end{aligned} \quad (2.18)$$

where the multiplicative correction to the purely perturbative contributions were determined up to corrections of the order $1/q^4$ or $\ln q/\mu$. Finally, putting together the defining relation eq. (2.8) and the results eqs. (2.18) we obtain

$$\begin{aligned} \alpha_T(\mu^2) &= \lim_{\Lambda \rightarrow \infty} \frac{g_0^2}{4\pi} F^2(\mu^2, \Lambda) G(\mu^2, \Lambda) \\ &= \lim_{\Lambda \rightarrow \infty} \frac{g_0^2}{4\pi} F^2(q_0^2, \Lambda) F_R^2(\mu^2, q_0^2) G(q_0^2, \Lambda) G_R(\mu^2, q_0^2) \\ &= \alpha_T^{\text{pert}}(q_0^2) F_{R,\text{pert}}^2(\mu^2, q_0^2) G_{R,\text{pert}}(\mu^2, q_0^2) \left(1 + \frac{9}{\mu^2} \frac{g_T^2(q_0^2) \langle A^2 \rangle_{R, q_0^2}}{4(N_C^2 - 1)} \right) \\ &= \alpha_T^{\text{pert}}(\mu^2) \left(1 + \frac{9}{\mu^2} \frac{g_T^2(q_0^2) \langle A^2 \rangle_{R, q_0^2}}{4(N_C^2 - 1)} \right), \end{aligned} \quad (2.19)$$

where $q_0^2 \gg \Lambda_{\text{QCD}}^2$ is some perturbative scale and the β -function, and its coefficients in eq. (2.13), of course describe the running of the perturbative part of the evolution, α_T^{pert} . The anomalous dimension for the Wilson coefficient,

$$\gamma_{A^2}(\alpha(\mu^2)) = \lim_{\Lambda \rightarrow \infty} \frac{d}{d \ln \mu^2} \ln Z_{A^2}(\mu^2, \Lambda^2) = -\gamma_0^{A^2} \frac{\alpha(\mu^2)}{4\pi} + \dots \quad (2.20)$$

where $A_R^2 = Z_{A^2}^{-1} A^2$, is neglected in eq. (2.19).

The leading logarithm contribution for the Wilson coefficient are incorporated as explained in [18], yielding:

$$\alpha_T(\mu^2) = \alpha_T^{\text{pert}}(\mu^2) \left(1 + \frac{9}{\mu^2} \left(\frac{\alpha_T^{\text{pert}}(\mu^2)}{\alpha_T^{\text{pert}}(q_0^2)} \right)^{1 - \gamma_0^{A^2}/\beta_0} \frac{g_T^2(q_0^2) \langle A^2 \rangle_{R, q_0^2}}{4(N_C^2 - 1)} \right), \quad (2.21)$$

where $\gamma_0^{A^2}$ can be taken from [20, 28] to give

$$1 - \frac{\gamma_0^{A^2}}{\beta_0} = 1 - \frac{105 - 8N_f}{132 - 8N_f} = \frac{9}{44 - \frac{8}{3}N_f}, \quad (2.22)$$

which agrees for $N_f = 0$ with the power of the logarithmic correction applied, and shown to have a negligible impact on α in [18]. We shall first apply formula eq. (2.21), approximated up to the four-loop level in perturbation and up to the leading-log in the OPE expansion, to describe the lattice data in the next sections. As already mentioned we postpone the use of four-loop Wilson coefficients [20] and the study of the impact of higher order operators to the end of section 4.

3 The lattice computation of the Taylor coupling

The following section is devoted to the computation of the running coupling in Taylor scheme, eq. (2.8), from the lattice. The results presented here are based on the gauge field configurations generated by the European Twisted Mass Collaboration (ETMC) with the tree-level improved Symanzik gauge action [29] and the twisted mass fermionic action [30] at maximal twist.

3.1 The lattice action

A very detailed discussion about the twisted mass and tree-level improved Symanzik gauge actions, and about the way they are implemented by ETMC, can be found in refs. [19,31–33]. Here, for the sake of completeness, we will present a brief reminder of the twisted action and the run parameters for the gauge configurations that will be exploited in the present work (See tab. 1).

The Wilson twisted mass fermionic lattice action for two flavours of mass degenerate quarks, reads (in the so called twisted basis [30,34])

$$S_{\text{tm}}^{\text{F}} = a^4 \sum_x \left\{ \bar{\chi}_x [D_{\text{W}} + m_0 + i\gamma_5 \tau_3 \mu_q] \chi_x \right\}, \quad (3.1)$$

$$D_{\text{W}} = \frac{1}{2} \gamma_\mu (\nabla_\mu + \nabla_\mu^*) - \frac{ar}{2} \nabla_\mu \nabla_\mu^*,$$

where m_0 is the bare untwisted quark mass and μ_q the bare twisted quark mass, τ_3 is the third Pauli matrix acting in flavour space and r is the Wilson parameter, which is set to $r = 1$ in the simulations. The operators ∇_μ and ∇_μ^* stand for the gauge covariant nearest neighbour forward and backward lattice derivatives. The bare quark mass m_0 is related as usual to the so-called hopping parameter κ , by $\kappa = 1/(8 + 2am_0)$. Twisted mass fermions are said to be at *maximal twist* if the bare untwisted mass is tuned to its critical value, m_{crit} . This is in practice done by setting the so-called untwisted PCAC mass to zero.

In the gauge sector the tree-level Symanzik improved gauge action (tlSym) [29] is applied. This action includes besides the plaquette term $U_{x,\mu,\nu}^{1 \times 1}$ also rectangular (1×2) Wilson loops $U_{x,\mu,\nu}^{1 \times 2}$. It reads

$$S_g = \frac{\beta}{3} \sum_x \left(b_0 \sum_{\substack{\mu,\nu=1 \\ 1 \leq \mu < \nu}}^4 \{1 - \text{ReTr}(U_{x,\mu,\nu}^{1 \times 1})\} + b_1 \sum_{\substack{\mu,\nu=1 \\ \mu \neq \nu}}^4 \{1 - \text{ReTr}(U_{x,\mu,\nu}^{1 \times 2})\} \right), \quad (3.2)$$

where $\beta \equiv 6/g_0^2$, g_0 being the bare lattice coupling and it is set $b_1 = -1/12$ (with $b_0 = 1 - 8b_1$ as dictated by the requirement of continuum limit normalization). Note that at $b_1 = 0$ this action becomes the usual Wilson plaquette gauge action. The run parameters for β and μ_q of the gauge configurations that will be exploited in the following can be found in tab. 1.

β	$a\mu_q$	Volume	Number of confs.
3.9	0.004	$24^3 \times 48$	120
	0.0064		20
	0.010		20
4.05	0.003	$32^3 \times 64$	20
	0.006		20
	0.008		20
	0.012		20
4.2	0.0065	$32^3 \times 64$	200

Table 1: Run parameters of the exploited data from ETMC collaboration.

3.2 The computation of the gluon and ghost Green functions

Applying eq. (2.8) demands to compute the gauge-fixed 2-point gluon and ghost Green functions from the lattice. To this goal, we exploited ETMC gauge configurations obtained for $\beta = 3.9$, $\beta = 4.05$ and $\beta = 4.2$ and a large variety of dynamical quark masses, fixed by the values of the μ_q parameter. The lattice gauge configurations are transformed to Landau gauge by minimising the following functional of the SU(3) matrices, $U_\mu(x)$,

$$F_U[g] = \text{Re} \left[\sum_x \sum_\mu \text{Tr} \left(1 - \frac{1}{N} g(x) U_\mu(x) g^\dagger(x + \mu) \right) \right] \quad (3.3)$$

with respect to the gauge transform g , by applying a combination of overrelaxation algorithm and Fourier acceleration³. This procedure does not avoid the possibility of lattice Gribov copies that, in any case, have been reported to have a nonsignificant influence beyond the lowest momenta. Then, the gauge field is defined as

$$A_\mu(x + \hat{\mu}/2) = \frac{U_\mu(x) - U_\mu^\dagger(x)}{2ia g_0} - \frac{1}{3} \text{Tr} \left(\frac{U_\mu(x) - U_\mu^\dagger(x)}{2ia g_0} \right) \quad (3.4)$$

where $\hat{\mu}$ indicates the unit lattice vector in the direction μ and g_0 is the bare coupling constant. The 2-gluon Green functions is computed in momentum space by

$$(G^{(2)})_{\mu_1 \mu_2}^{a_1 a_2}(p) = \langle A_{\mu_1}^{a_1}(p) A_{\mu_2}^{a_2}(-p) \rangle \quad (3.5)$$

where $\langle \dots \rangle$ indicates the Monte-Carlo average and where

$$A_\mu^a(p) = \frac{1}{2} \text{Tr} \left[\sum_x A_\mu(x + \hat{\mu}/2) \exp(ip(x + \hat{\mu}/2)) \lambda^a \right] \quad (3.6)$$

³We end when $|\partial_\mu A_\mu|^2 < 10^{-11}$ and when the spatial integral of A_0 is constant in time to better than 10^{-6} .

λ^a being the Gell-Mann matrices and the trace being taken in the 3×3 color space.

On the other hand, the ghost propagator is also computed in Landau gauge,

$$(F^{(2)})^{ab}(x-y) \equiv \langle (M^{-1})_{xy}^{ab} \rangle, \quad (3.7)$$

as the inverse of the Faddeev-Popov operator, that is written as the lattice divergence,

$$M(U) = -\frac{1}{N} \nabla \cdot \tilde{D}(U) \quad (3.8)$$

where the operator \tilde{D} acting on an arbitrary element of the Lie algebra, η reads:

$$\tilde{D}(U)\eta(x) = \frac{1}{2} (U_\mu(x)\eta(x+\mu) - \eta(x)U_\mu(x) + \eta(x+\mu)U_\mu^\dagger - U_\mu^\dagger(x)\eta(x)) . \quad (3.9)$$

More details on the lattice procedure for the inversion of Faddeev-Popov operator can be found in [35].

3.3 On the treatment of lattice artefacts

The lattice estimates of the Landau-gauge propagators through eqs. (3.5,3.7), after Fourier transforming the ghost correlator and appropriate projection of both as indicated by eq. (2.1), lead to the determination of ghost and gluon dressing functions to be used in eq. (2.8). Both dressing functions are dimensionless lattice correlation functions (let us note both as $Q \equiv F, G$) that, because of general dimensional arguments, depend on the lattice momentum $a p_\mu$, where

$$p_\mu = \frac{2\pi n}{Na} \quad n = 0, 1, \dots, N, \quad (3.10)$$

and on the strong interaction scale Λ_{QCD} . Anticipating on the averaging over hypercubic orbits and on the treatment of hypercubic lattice artefacts we get $Q \equiv Q(a^2 p^2, a^2 \Lambda_{\text{QCD}}^2)$. Our choice for the lattice action ensures that the discretization artefacts due to the lattice are $\mathcal{O}(a^2)$, where a is the lattice spacing.

Thus, the running coupling in Taylor scheme is obtained by

$$\alpha_T(\mu^2) = \lim_{a \rightarrow 0} \frac{g(a^2)}{4\pi} F^2(a^2 p^2, a^2 \Lambda_{\text{QCD}}^2) G(a^2 p^2, a^2 \Lambda_{\text{QCD}}^2), \quad (3.11)$$

where taking the limit of a vanishing lattice spacing indeed implies the proper elimination of lattice artefacts.

3.3.1 Hypercubic $H(4)$ -extrapolation

A first kind of artefacts that can be systematically cured [36, 37] are those due to the breaking of the rotational symmetry of the Euclidean space-time when using an hypercubic lattice, where this symmetry is restricted to the discrete $H(4)$ isometry group. It is convenient to compute first the average of any dimensionless lattice quantity $Q(ap_\mu)$ over every orbit of the group $H(4)$. In general several orbits of $H(4)$ correspond to one value of p^2 . Defining the $H(4)$ invariants

$$p^{[4]} = \sum_{\mu=1}^4 p_\mu^4 \quad p^{[6]} = \sum_{\mu=1}^6 p_\mu^6 \quad (3.12)$$

it happens that the orbits of $H(4)$ are labelled ⁴ by the set $p^2, a^2 p^{[4]}, a^4 p^{[6]}$. In the continuum limit the effect of $a^2 p^{[4]}, a^4 p^{[6]}$ vanishes. We can thus define the quantity $Q(ap_\mu)$ averaged over $H(4)$ as

$$Q(a^2 p^2, a^4 p^{[4]}, a^6 p^{[6]}, a^2 \Lambda_{\text{QCD}}^2). \quad (3.13)$$

If the lattice spacing is small enough such that $\epsilon = a^2 p^{[4]}/p^2 \ll 1$, the dimensionless lattice correlation function defined in eq. (3.13) can be expanded in powers of ϵ :

$$Q(a^2 p^2, a^4 p^{[4]}, a^6 p^{[6]}, a^2 \Lambda_{\text{QCD}}^2) = Q(a^2 p^2, a^2 \Lambda_{\text{QCD}}^2) + \left. \frac{dQ}{d\epsilon} \right|_{\epsilon=0} a^2 \frac{p^{[4]}}{p^2} + \dots \quad (3.14)$$

$H(4)$ methods are based on the appearance of a $\mathcal{O}(a^2)$ corrections driven by a $p^{[4]}$ term. The basic method is to fit from the whole set of orbits sharing the same p^2 the coefficient $dQ/d\epsilon$ and get the extrapolated value of Q , free from $H(4)$ artefacts. If we further assume that the coefficient

$$R(a^2 p^2, a^2 \Lambda_{\text{QCD}}^2) = \left. \frac{dQ(a^2 p^2, 0, 0, a^2 \Lambda_{\text{QCD}}^2)}{d\epsilon} \right|_{\epsilon=0}$$

has a smooth dependence on $a^2 p^2$ over a given momentum window, we can expand R as $R = R_0 + R_1 a^2 p^2$ and make a global fit in a momentum window between $(p - \delta, p + \delta)$ to extract the extrapolated value of Q for the momenta p in the window, and shift to the next window etc. This procedure of fitting with windows is somehow different from the basic one, since the extrapolation does not rely on any particular assumption for the functional form of R . On the other, the systematic error coming from the extrapolation can be estimated by modifying the width of the fitting window.

It is worthwhile to mention that we considered in this work anisotropic lattice of the type $L^3 \times T$, with $T = 2L$. This finite volume effect reduces the $H(4)$ lattice symmetry to $H(3)$. Deviations from $H(4)$ are to be expected in the long-distance physics. But ultraviolet physics should not be affected. As far as we are interested in the high-momentum regime, we will assume the previous treatment of the lattice artefacts to be valid.

⁴On totally general grounds, any $H(4)$ -invariant polynome can be written only in terms of the four invariants $p^{[2i]}$ with $i = 1, 2, 3, 4$ [36, 37]. As a consequence of the upper cut for momenta, the first three of these invariants suffice to label all the orbits we deal with and hence any presumed dependence on $p^{[8]}$ is neglected.

3.3.2 Quark mass artefacts

In this section we will consider the influence of the dynamical quark masses. We will argue that this is a $\mathcal{O}(a^2\mu_q^2)$ effect and therefore that it is a lattice artefact.

Following the treatment described in the previous section, we have calculated the $H(4)$ -free ghost and gluon dressing functions, that we shall denote in the following by \widehat{F}, \widehat{G} . These dressing functions can be combined in order to calculate the $H(4)$ -free lattice coupling through eq. (3.11).

In the analysis performed ref. [18] by exploiting “quenched” configurations, a pretty good scaling of α_T was found, computed at different β 's from eq. (3.11), once one parameter describing the lattice spacing ratios had been fitted. This seems to imply that the residual $\mathcal{O}(a^2p^2)$ artefacts are negligible for the “quenched” coupling constant in Taylor scheme after $H(4)$ -extrapolation has been performed. Of course $\mathcal{O}(a^2\Lambda_{\text{QCD}}^2)$ artefacts may still be hidden in the matching coefficient between lattice spacings.

It is worth pointing that all the divergent contributions appearing for the dressing functions or the bare coupling when the lattice spacing vanishes cancel when combined in eq. (3.11).

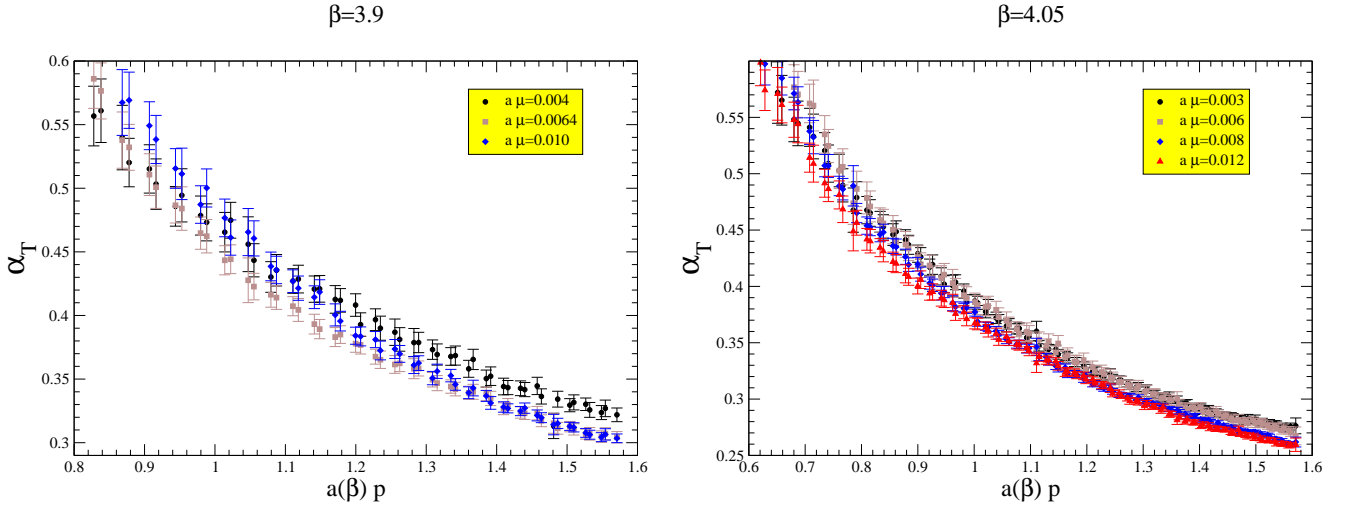


Figure 1: The Taylor couplings estimates through eq. (3.11), after $H(4)$ -extrapolation, at $\beta = 3.9$ for $\mu_q = 0.004, 0.0064, 0.010$ (left-hand plots) and at $\beta = 4.05$ for $\mu_q = 0.003, 0.006, 0.008, 0.012$ (right-hand plots).

However, when analyzing “unquenched” lattice configurations, one should keep in mind that one additional mass scale, the dynamical quark mass, is playing a role. In Fig. 1 one can see the Taylor coupling after hypercubic extrapolation for different μ_q at fixed $\beta = 3.9$ and 4.05 . Indeed, a dependence in μ_q is clearly seen. If it is an artefact the dependence should be in $a^2\mu_q^2$. If it is an effect in the continuum it should be some unknown function of the physical mass μ_q . Trying

an $\mathcal{O}(a^2\mu_q^2)$ dependence, we write the expansion :

$$\begin{aligned}\widehat{\alpha}_T(a^2p^2, a^2\mu_q^2) &= \frac{g_0^2(a^2)}{4\pi} \widehat{G}(a^2p^2, a^2\mu_q^2) \widehat{F}^2(a^2p^2, a^2\mu_q^2) \\ &= \widehat{\alpha}_T(a^2p^2, 0) + \frac{\partial \widehat{\alpha}_T}{\partial (a^2\mu_q^2)}(a^2p^2) a^2\mu_q^2 + \dots;\end{aligned}\quad (3.15)$$

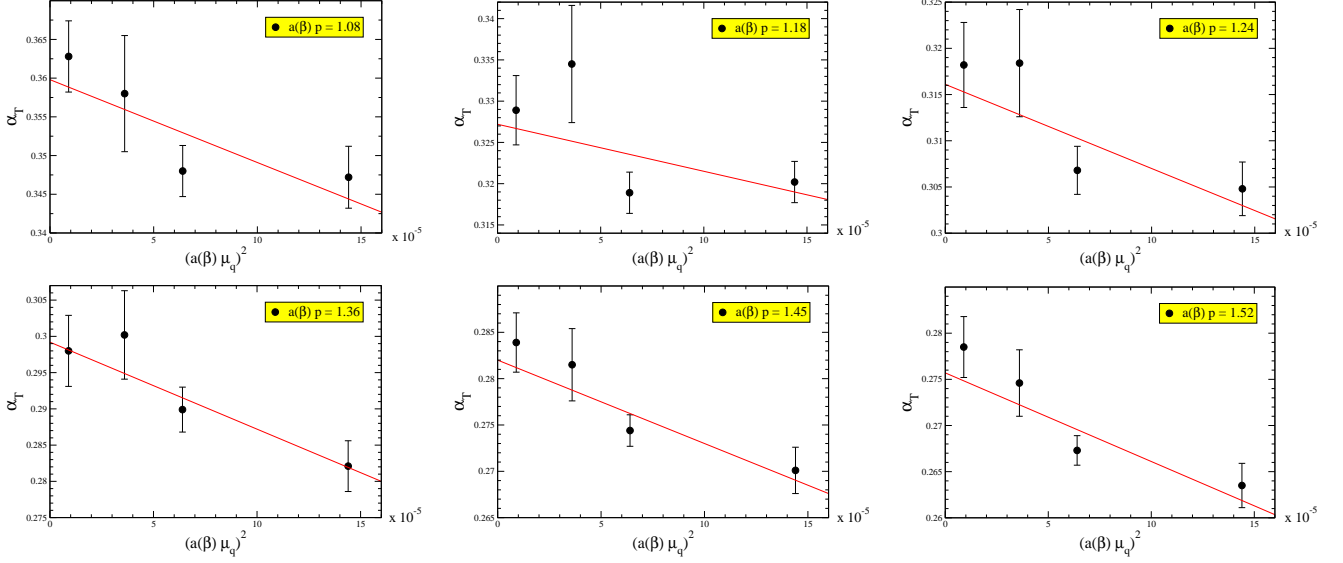


Figure 2: We plot the values of the Taylor coupling at $\beta = 4.05$, computed for some representative values of the lattice momentum, $a(4.05)p = 1.08, 1.18, 1.24, 1.36, 1.45, 1.52$, in terms of $a^2(4.05)\mu_q^2$ and show the suggested linear extrapolation at $a^2\mu_q^2 = 0$.

Provided that the first-order expansion in eq. (3.15) is reliable, a linear behaviour on $a^2\mu_q^2$ has to be expected for the lattice estimates of $\widehat{\alpha}_T$ for any fixed lattice momentum computed from simulations at any given β and several values of μ_q . We explicitly check this linear behaviour to occur for the results from our $\beta = 4.05$ and $\beta = 3.9$ simulations and show in Fig. 2 some plots of $\widehat{\alpha}_T$ computed at $\beta = 4.05$ (where four different quark masses are available) for some representatives lattice momenta in terms of $a^2\mu_q^2$. We thus write the Taylor expansion as and after neglecting the $\mathcal{O}(a^4)$ contributions get

$$\widehat{\alpha}_T(a^2p^2, a^2\mu_q^2) = \alpha_T(p^2) + R_0(a^2p^2) a^2\mu_q^2, \quad (3.16)$$

where $R_0(a^2p^2)$ is defined as

$$R_0(a^2p^2) \equiv \frac{\partial \widehat{\alpha}_T}{\partial (a^2\mu_q^2)} \quad (3.17)$$

In fig. 3, we plot $R_0(a^2p^2)$ as a function of ap computed for the four lattices simulations at $\beta = 4.05$ with different quark masses and for the three ones at $\beta = 3.9$ (see tab. 1). Indeed, it can be seen that a constant behaviour appears to be achieved for $p \geq p_{\min} \simeq 2.8$ GeV. We will not risk an interpretation of the data below $(ap)_{\min}$. The striking observation here is that above p_{\min} both lattice spacings exhibit a fairly constant $R_0(a^2p^2)$ and a good enough scaling between both β 's.

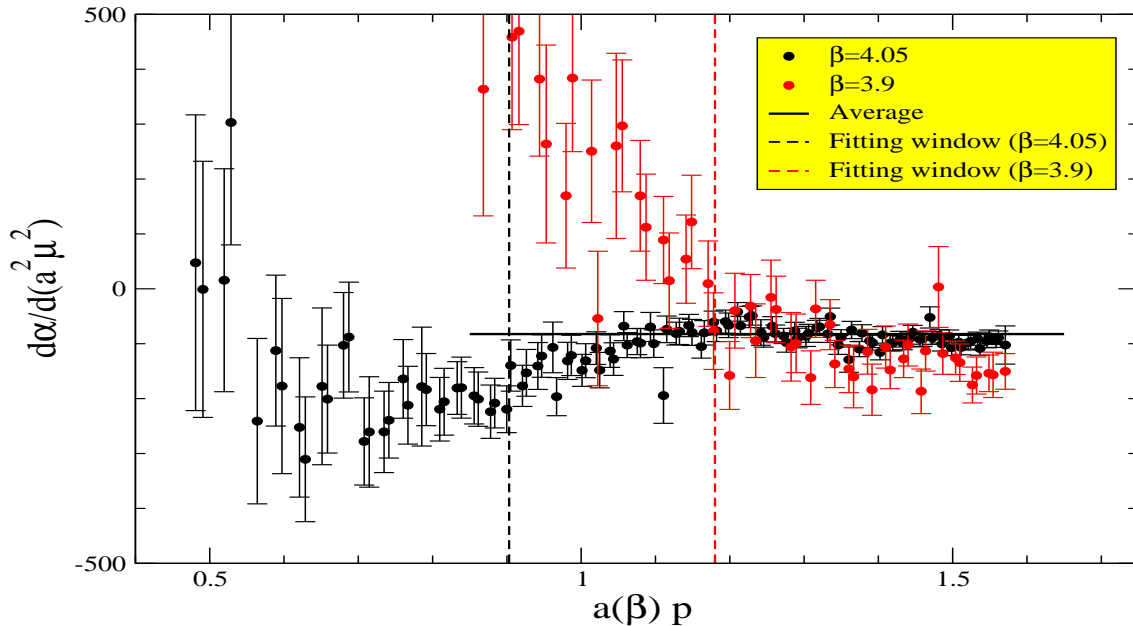


Figure 3: The slopes for the mass squared extrapolation in terms of ap computed for the four lattices simulations at $\beta = 4.05$ ($32^3 \times 64$) with $a\mu_q = 0.003, 0.006, 0.008, 0.012$ and for the three ones at $\beta = 3.9$ ($24^3 \times 48$) with $a\mu_q = 0.004, 0.0064, 0.010$. The supposed constant behaviour appear to be reached when lattice volume effects become negligible for each simulation.

The analysis of the slopes (see fig. 3) leaves us with both a fair estimate of R_0 above 2.8 GeV, $R_0 \sim -0.9 \cdot 10^2$, and an intrinsic definition for the momentum window where eq. (3.16) can be applied to extrapolate at any momentum. Thus, after the extrapolation with the previously obtained R_0 down to vanishing $a\mu_q$, one obtains the three estimates for the running coupling at $\beta = 3.9, 4.05, 4.2$ plotted in terms of the momentum in lattice units, ap , in fig. 4.(a), which shows a very smooth running behaviour. These are the lattice estimates for the coupling to be confronted to the analytical prediction given by eq. (2.21).

The fact that R_0 with our present data goes to the same constant for both β 's, leads us to consider that the μ_q dependence of α is mainly a lattice artefact (else it should be a function of μ_q and not of $a\mu_q$). The slope R_0 is not small. We did not expect this. It has to be seriously considered as it affects the result on $\Lambda_{\overline{MS}}$. The slope being negative, the extrapolation to vanishing

$a\mu_q$ leads to a larger value for $\Lambda_{\overline{\text{MS}}}$ than if we had estimated it at finite $a\mu_q$. We shall see that this effect is of the order of an increase of 40 MeV on $\Lambda_{\overline{\text{MS}}}$.

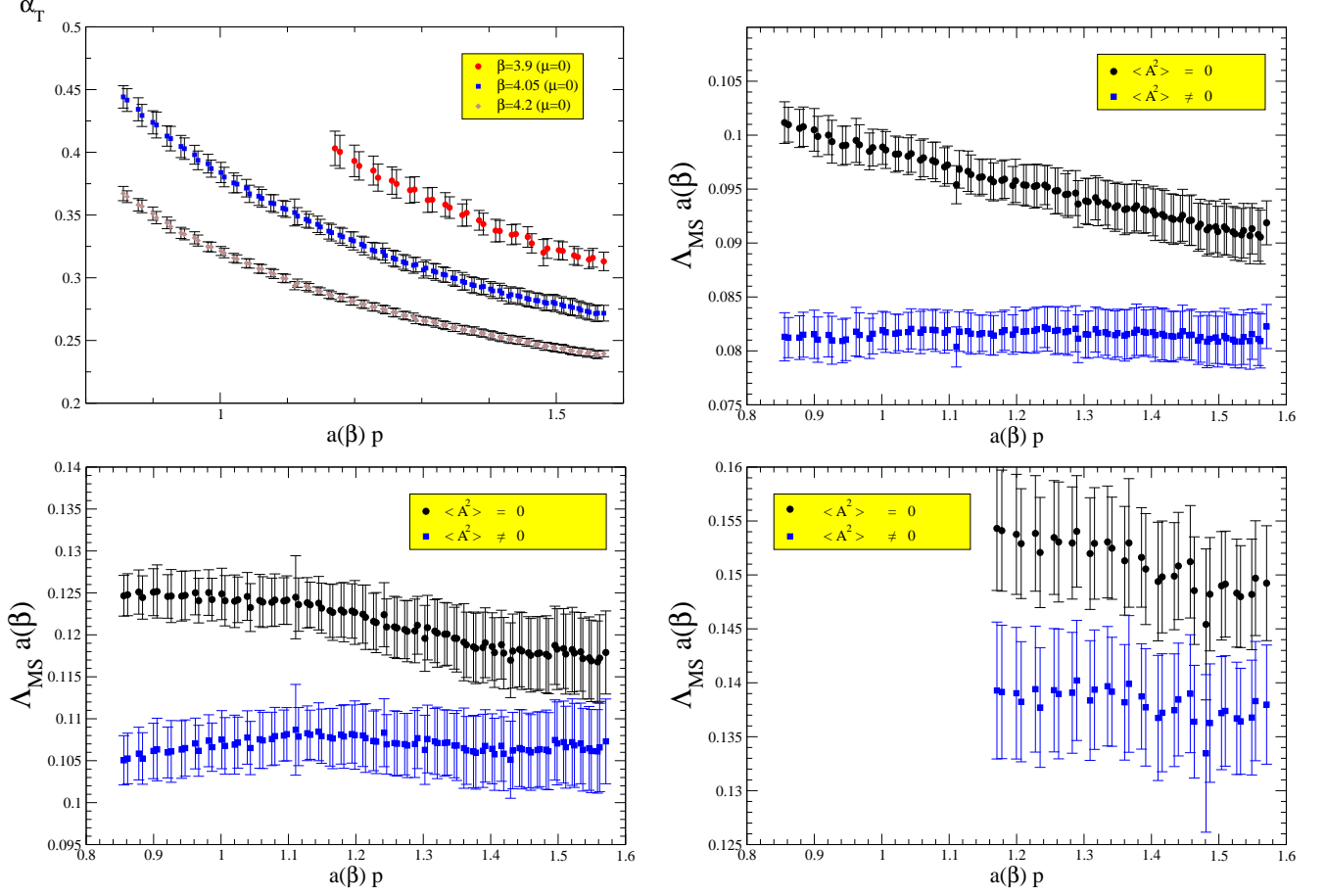


Figure 4: Left-hand plot (up): The Taylor coupling, free of $H(4)$ and mass-quarks artefacts, computed by applying eq. (3.16) for the three $\beta = 3.9, 4.05, 4.2$ and plotted in terms of the lattice momentum $a(\beta)p$. The three other plots show $\Lambda_{\overline{\text{MS}}}$ in lattice units, computed by the inversion of eq. (4.2) with the lattice couplings plotted in the upper left-hand plot, for $\beta = 4.2$ (upper right), $\beta = 4.05$ (bottom left) and $\beta = 3.9$ (bottom right); the black circles are for a perturbative inversion (with zero gluon condensate) and blue squares are computed with the best-fit of the gluon condensate (see the text).

Taking into account the effects due to dynamical quarks in a global analysis of the lattice determinations is among the main results of this paper. This will lead to a proper extrapolation to the continuum limit.

4 Computing $\Lambda_{\overline{\text{MS}}}$ and the gluon condensate

In this section, following [18], we will apply a “plateau”-procedure exploiting eq. (2.21) to get a reliable estimate of the Λ_{QCD} -parameter from the Taylor running coupling constant computed as explained in the previous section from lattice simulations with $N_f = 2$ dynamical quark flavors.

4.1 Looking for the “plateau”

In fig. 4, we show the estimates of $\Lambda_{\overline{\text{MS}}}$ obtained when interpreting the lattice coupling computed from eq. (3.11) for $\beta = 3.9, 4.05, 4.2$ for all momenta inside the window where the slope for the μ_q -extrapolation behaves as a constant, i.e. for $p \geq p_{\text{min}} \simeq 2.8$ GeV, up to our chosen lattice upper bound ⁵ of $ap < 1.6$. The estimate of $\Lambda_{\overline{\text{MS}}}$ is done first (black circles) thanks to the *inverted* four-loop perturbative formula for the coupling, eq. (2.11). These estimates systematically decrease as the lattice momentum increases, while if we were in the perturbative region it should be a constant as $\Lambda_{\overline{\text{MS}}}$ is, by definition, a constant in the perturbative expansion. This clearly reveals the necessity of applying the non-perturbative formula including power corrections, eq. (2.21), with a non-zero gluon condensate. This is also done in fig. 4, where the same is plotted but inverting instead the non-perturbative formula (blue squares). The value of the gluon condensate has been determined by requiring a “plateau” to exist over the total momenta window. More precisely, one requires the best-fit to a constant of the estimates of $\Lambda_{\overline{\text{MS}}}$, in lattice units, in terms of the lattice momentum,

$$(x_i, y_i) \equiv (ap_i, \Lambda_i) , \quad (4.1)$$

where, of course, i runs to cover all the lattice estimates of the coupling inside the defined window and where Λ_i is obtained by inverting ⁶

$$\alpha_T^{\text{pert}} \left(\log \frac{a^2 p_i^2}{\Lambda_i^2} \right) = \frac{\hat{\alpha}_T(a^2 p_i^2, 0)}{1 + \frac{c}{a^2 p_i^2}} , \quad (4.2)$$

with α_T^{pert} given by the perturbative four-loop formula eq. (2.11), $\hat{\alpha}_T(a^2 p_i^2, 0)$ taken from the extrapolation of the lattice couplings by eq. (3.16) and c resulting from the best-fit (it appeared written in terms of the gluon condensate in eq. (2.19)) of Λ_i to a constant. Thus, Λ_i is required to reach a “plateau”, behaving as a constant when i runs, in terms of the lattice momentum.

This procedure leaves us with estimates of $\Lambda_{\overline{\text{MS}}}$ and the gluon condensate (computed from the best-fit determination of c), expressed in lattice units, for any β . However, we will take this as a striking illustration of the necessity of including non-perturbative power corrections in the analysis (see fig. 4) but we will only report the results obtained in the next section when a global fitting strategy will be applied to our μ_q -extrapolated lattice data for the three different β 's.

⁵Above some value of ap the lattice artefacts become overwhelming. One must choose an upper bound, this choice being to some extent arbitrary.

⁶For the sake of simplification we are using here the tree level value for the Wilson coefficient of the dimension-2 condensate, i.e. a constant ; higher orders will be considered in the next sections.

4.2 Global fit and the calibration of lattice spacing

The running of α_T given by the combination of Green functions in eq. (3.11) and the extrapolation through eq. (3.16), provided that we are not far from the continuum limit and discretization errors are treated properly, depend only on the momentum (except, maybe, finite volume errors at low momenta). The supposed scaling of the Taylor coupling implies for the three curves plotted in fig. 4.(a) to match to each other after the appropriate conversion of the momentum (in x-axis) from lattice to physical units, with the multiplication by the lattice spacing at each β . Thus, we can apply the ‘‘plateau’’-method described in the previous subsection for the three β ’s all at once by requiring the minimisation of the total χ^2 :

$$\chi^2 \left(a(\beta_0)\Lambda_{\overline{\text{MS}}}, c, \frac{a(\beta_1)}{a(\beta_0)}, \frac{a(\beta_2)}{a(\beta_0)} \right) = \sum_{j=0}^2 \sum_i \frac{\left(\Lambda_i(\beta_j) - \frac{a(\beta_j)}{a(\beta_0)} a(\beta_0)\Lambda_{\overline{\text{MS}}} \right)^2}{\delta^2(\Lambda_i)}; \quad (4.3)$$

where the sum over j covers the sets of coupling estimates for the three β ’s ($\beta_0 = 3.9$, $\beta_1 = 4.05$, $\beta_2 = 4.2$), the index i runs to cover the fitting window defined, as previously explained, through the slope analysis ⁷ and $\Lambda_i(\beta_j)$ is again obtained for any β_j by requiring

$$\alpha_T^{\text{pert}} \left(\log \frac{a^2(\beta_j)p_i^2}{\Lambda_i^2(\beta_j)} \right) \left(1 + \frac{c}{a^2(\beta_j)p_i^2} \left(\frac{a(\beta_j)}{a(\beta_0)} \right)^2 \left(\frac{\log \frac{a^2(\beta_j)p_i^2}{\Lambda_i^2(\beta_j)}}{\log \frac{a^2(\beta_0)q_0^2}{\Lambda_i^2(\beta_j)}} \right)^{-\frac{27}{116}} \right) = \hat{\alpha}_T(a^2(\beta_j)p_i^2, 0) \quad (4.4)$$

where now we apply the OPE formula including the leading logarithm correction for the Wilson coefficient, eq. (2.21), with α_T^{pert} given by the perturbative four-loop formula, eq. (2.11), and where $a(\beta_0)q_0 = 4.5$ (this means $q_0 \approx 10$ GeV). The errors for the extrapolated couplings are estimated by jackknife analysis and properly propagated through the perturbative inversion to give $\delta(\Lambda_i)$. The function χ^2 is minimised over the functional space defined by the four parameters that are explicitly put in arguments for eq. (4.3)’s l.h.s.: $a(\beta_0)\Lambda_{\overline{\text{MS}}}$, c , $\frac{a(\beta_1)}{a(\beta_0)}$, $\frac{a(\beta_2)}{a(\beta_0)}$. Thus we obtain all at once $\Lambda_{\overline{\text{MS}}}$ and the gluon condensate, in units of the lattice spacing for $\beta_0 = 3.9$, and the ratios of lattice spacings for our three simulations after the extrapolation to the limit $\mu_q \rightarrow 0$ (see tab. 2). The errors are calculated again by jackknife analysis.

The ratios of lattice spacings can be applied to express the momenta for all the three sets of coupling estimates plotted in fig. 4 (upper left-handed plot) in units of the lattice spacing at $\beta = 3.9$. Thus they indeed match each other and fit pretty well to the analytical prediction given by eq. (2.21) with the best-fit parameters for $\Lambda_{\overline{\text{MS}}}$ and the gluon condensate, in units of $1/a(3.9)$

⁷In the case of $\beta_2 = 4.2$, as only the simulation for one quark mass, $\mu_q = 0.0065$, is exploited, one extrapolates by applying the slope R_0 computed for $\beta_0 = 3.9$ and $\beta_1 = 4.05$ all the coupling estimates obtained inside the same lattice-momentum window determined for $\beta_1 = 4.05$. So we do because simulations at both $\beta_1 = 4.05$ and $\beta_2 = 4.2$ were performed in $32^3 \times 64$ lattices and the impact of volume effects were supposed to determine the lower bound of the fitting window.

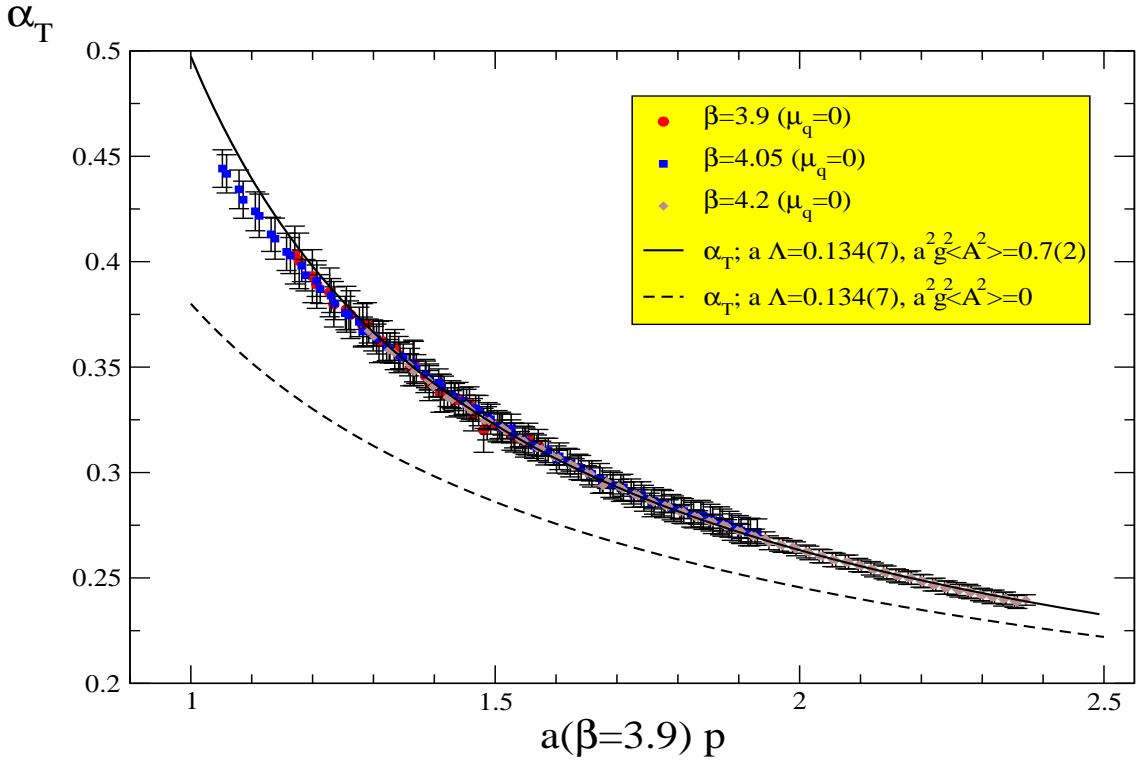


Figure 5: The scaling of the Taylor coupling computed by applying eq. (3.16) for the three $\beta = 3.9, 4.05, 4.2$ is shown. The lattice momentum, $a(\beta)p$ in the x-axis, is converted to a physical momentum in units (the same for the three β 's) of $a(3.9)^{-1}$. For so to do, the ratios of the lattice spacings must be applied. The solid curve is the non-perturbative prediction given by eq. (2.21) with the best-fit parameters for $\Lambda_{\overline{\text{MS}}}$ and the gluon condensate, and the dotted one is the same but with zero gluon condensate.

(see tab. 2), as can be seen in the plot of fig. 5. The quality for the fits drastically deteriorates as data below $a(3.9)p \simeq 1.2$ are included, whichever value results for the gluon condensate. Thus, a fitting window excluding those data are applied in obtaining the best-fit parameters in tab. 2 and the best-fit curve in fig. 5 which clearly detaches from the data below such a lower bound.

4.3 The contribution from the Wilson coefficient higher orders

The Wilson coefficients for gluon and ghost propagators have been very recently obtained at four-loop level [20]. As it is shown in appendix, by exploiting the results of this ref. [20], the four-loop OPE formula for the T-scheme coupling for $N_f = 2$ can be obtained by replacing in eq. (2.21):

$$\begin{aligned}
g_T^2(q_0^2) &\rightarrow g_T^2(q_0^2) \left(1 + 1.2932 \alpha(\mu^2) + 1.9363 \alpha^2(\mu^2) + 3.8296 \alpha^3(\mu^2) \right) \\
&\times \left(1 - 0.7033 \alpha(q_0^2) - 0.3652 \alpha^2(q_0^2) + 0.0051 \alpha^3(q_0^2) \right)
\end{aligned} \tag{4.5}$$

	This paper	String tension
$a(3.9)/a(4.05)$	1.224(23)	1.255(42)
$a(3.9)/a(4.2)$	1.510(32)	1.558(52)
$a(4.05)/a(4.2)$	1.233(25)	1.241(39)
$\Lambda_{\overline{\text{MS}}}a(3.9)$	0.134(7)	
$g^2\langle A^2\rangle a^2(3.9)$	0.70(23)	

Table 2: Best-fit parameters for the ratios of lattice spacings, $\Lambda_{\overline{\text{MS}}}$ and the gluon condensate (for which $a(3.9)q_0 = 4.5$ is chosen). For the sake of comparison, we also quote the results from [38] that were obtained by computing the hadronic quantity, $r_0/a(\beta)$, and applying to it a chiral extrapolation.

where $\alpha = \alpha_T^{\text{pert}}$ and q_0^2 is the renormalization momentum for the local operator A^2 (see next eq. (A.9) and compare with eq. (2.21) that only incorporates the leading logarithmic contribution) which we fixed, as previously indicated, by requiring: $a(3.9)q_0 = 4.5$.

Then, we can repeat the analysis of previous sections, after the replacement prescribed in eq. (4.5), and obtain the results collected in tab. 3. Thus, a strong stability results from the fits for the estimates of $\Lambda_{\overline{\text{MS}}}$ (all of them being compatible within the statistical uncertainties and varying less than a 2.3 %) and a fairly convergent behaviour for that of the gluon condensate which, computed with the one-loop Wilson coefficient, clearly borrows something from next-to-leading contributions.

	One loop	Two loops	Three loops	Four loops
$\Lambda_{\overline{\text{MS}}}a(3.9)$	0.134(7)	0.136(7)	0.137(7)	0.138(7)
$g^2\langle A^2\rangle a^2(3.9)$	0.70(23)	0.52(18)	0.44(14)	0.39(14)

Table 3: Best-fit parameters for $\Lambda_{\overline{\text{MS}}}$ and the gluon condensate (for which $a(3.9)q_0 = 4.5$ is chosen) by applying a OPE formula including the logarithmic corrections for the Wilson coefficient at one, two, three and four loop order. No difference is seen for the ratios of lattice spacings.

4.4 Discussing the systematical uncertainties

The main sources of systematical uncertainties affecting the determination of the best-fit parameters ($\Lambda_{\overline{\text{MS}}}$, the non-perturbative gluon condensate and the ratios of lattice spacings) of the matching previously described are expected to come from the truncation of the perturbative series for the theoretical prediction of the coupling in eq. (2.21), the possible effect of higher-orders in the OPE expansion and from the finite volume effects in lattice simulations. We will pay attention in the following to these error sources.

4.4.1 Volume effects

As can be seen in tab. 1, we exploited lattice simulations in volumes $24^3 \times 48$ at $\beta = 3.9$ and $32^3 \times 64$ at $\beta = 4.05$ and 4.2 . In the case of $\beta = 4.2$, in order to spare computing time, we use a volume smaller than what is usually needed to measure hadronic quantities (in particular, a $48^3 \times 96$ lattice at $\beta = 4.2$ and $a\mu_q = 0.002$ is required), relying on the hope that, being interested in ultraviolet quantities, the finite volume effects will be reduced. One expects that the smaller the product of momentum and lattice size, the larger is the volume-effect impact. Indeed, we introduced a lattice momentum cut, $a(\beta)p_{\min}$, when we studied the quark-mass extrapolation, which the slopes for the mass squared extrapolation detached below from the constant behaviour, and we interpreted this as a possible volume effect. Furthermore, in fig. 5, no impact of any remaining volume effect on the determination of the coupling is seen: the impressive scaling shown by the results from our three simulations in fig 5 seems to confirm that we are finally left with no important volume effect.

4.4.2 Three-loop versus four-loop confrontation

A standard way to estimate the effect of perturbative-series truncation is to repeat the analysis described in previous sections but applying instead a three-loop formula for the perturbative inversion. If this is done, one obtains the results collected in tab. 4.

	Four loops	Three loops
$a(3.9)/a(4.05)$	1.224(23)	1.229(23)
$a(3.9)/a(4.2)$	1.510(32)	1.510(29)
$a(4.05)/a(4.2)$	1.233(26)	1.234(25)
$\Lambda_{\overline{\text{MS}}}a(3.9)$	0.134(7)	0.125(6)
$g^2\langle A^2\rangle a^2(3.9)$	0.70(23)	0.80(20)

Table 4: Best-fit parameters for the ratios of lattice spacings, $\Lambda_{\overline{\text{MS}}}$ and the gluon condensate (for which $a(3.9)q_0 = 4.5$ is chosen).

Then, we can conclude that no noticeable impact from the perturbative truncation is resulting on the determination of the ratios of lattice spacing. Nevertheless, a systematic uncertainty of roughly a 7 % can be estimated from the discrepancy of the three and four-loops estimates for the $\Lambda_{\overline{\text{MS}}}$. Analogously, the determination of the gluon condensate is affected by a correction of the order of 13 %.

4.4.3 The impact of higher-orders in the OPE expansion

We previously paid attention to the comparison of the best-fit results when applying Wilson coefficients for the OPE expansion at different loop-orders (see tab. 3). We then concluded that

the different estimates of $\Lambda_{\overline{\text{MS}}}$ differ from each other less than a 2.3 %, while those for the gluon condensate fairly converge as the loop-order increases to roughly one half of the one-loop result.

On the other hand, as previously explained, the quality for the fits drastically deteriorates as data below $a(3.9)p \simeq 1.2$ are considered (the χ^2 becomes of the order of four times larger). This could be an indication of the impact of OPE higher power corrections that could be simply parameterized as

$$\alpha_{T,P4}(\mu^2) = \alpha_T(\mu^2) + \frac{c_4}{\mu^4}, \quad (4.6)$$

where α_T is given by eq. (2.21) and c_4 is a constant encoding all the information coming from the condensates of higher-dimension operators and the Wilson coefficients (their anomalous dimension is thus neglected). If we try a fit with eq. (4.6) to the lattice data, good-quality fits are obtained for negative values of c_4 , of the order of -0.1 , while the positive estimated contribution of the gluon condensate increases drastically. The fitting function with or without the c_4/μ^4 turn out to be very close to one another over the whole momentum window. In other words there is a valley in the parameter space in which both the $1/\mu^4$ and the $1/\mu^2$ coefficients vary in an anticorrelated way without any significant change of the value of fitting function. Furthermore, including the c_4/μ^4 term increases drastically the errors. $\Lambda_{\overline{\text{MS}}}$ is also correlated with the other two parameters: it decreases when c_4/μ^4 decreases below zero, by about 10 % from the fit without c_4/μ^4 term and the fit with it.

Our conclusion is that the fit with c_4/μ^4 is extremely unstable. We therefore decide not to include it in our fits. The resulting systematic uncertainties is not larger than $\sim 10\%$ on $\Lambda_{\overline{\text{MS}}}$. The estimate of the gluon condensate may be more severely affected. But, as shown in the quenched case [18], the estimates of the gluon condensate stemming from different quantities, when neglecting c_4/μ^4 terms, are quite compatible. This would not be possible if the dimension-four operators, with different Wilson coefficients for every quantity, were playing a significant role. We remain thus rather confident in our estimate of $\langle A^2 \rangle$. What should be stressed here is that *the necessity of a positive non perturbative contribution is unavoidable, and that it is well taken into account by the dominant dimension-two $\langle A^2 \rangle$ condensate.*

4.5 Conversion to physical units and quark mass effect

In this section, we will apply the results for the lattice spacings at $\beta = 3.9, 4.05$ and 4.2 obtained in ref. [38] through a very exhaustive investigation of the light meson physics using maximally twisted mass fermions for $N_f = 2$ degenerated quark flavours (the gauge configurations we use in this work were part of the data ensembles generated by ETMC and analysed in ref. [38]). The physical scale is given by requiring $f_\pi = 130.7$ MeV as also done in [31]. We first computed the ratios of those lattice spacings obtained in ref. [38] and compared them with the ones obtained in this paper in tab. 2. The agreement is indeed remarkable. Then, by applying the result [38]

$$a(3.9) = 0.0801(14) \text{ fm}, \quad (4.7)$$

to convert into physical units our estimates of $\Lambda_{\overline{\text{MS}}}$ and the gluon condensate (see tab. 2), the final results are:

$$\begin{aligned}\Lambda_{\overline{\text{MS}}} &= (330 \pm 23 \pm 22_{-33}) \times \left(\frac{0.0801 \text{ fm} \cdot 130.7 \text{ MeV}}{a(3.9) f_\pi} \right) \text{ MeV} , \\ g^2(q_0^2) \langle A^2 \rangle_{q_0} &= (4.2 \pm 1.5 \pm 0.7^{+?}) \times \left(\frac{0.0801 \text{ fm} \cdot 130.7 \text{ MeV}}{a(3.9) f_\pi} \right)^2 \text{ GeV}^2 ;\end{aligned}\quad (4.8)$$

where we first quote the purely statistical errors, where the one from the lattice size determination in ref. [38] has been properly into account, and then the main systematical uncertainties which were detailed in the previous subsection and that, as explained, mainly tend to increase the gluon condensate and to decrease the value of $\Lambda_{\overline{\text{MS}}}$. In particular, for the gluon condensate, the contribution to the uncertainty of higher powers in OPE expansion, although unequivocally increasing its size, is very hard to be estimated (as discussed in the previous section) and we explicitly indicated this by the addition of a question mark in the upper systematical errors of eq. (4.8). It should be also remembered that $q_0 = 4.5 a(3.9)^{-1} = 11.1 \text{ GeV}$. In ref. [38], the lattice spacings result from combined fits including several lattice simulations at different β 's, after chiral extrapolations on the quark mass, where the physical scale is fixed by $f_\pi = 130.7 \text{ MeV}$. In particular, eq. (4.7) and the ratios we presented for the sake of comparison in tab. 2, were obtained in that ref. [38] through a combined fit including $\beta = 3.9, 4.05$ and 4.2 , but results obtained through combined fits including either $\beta = 3.8, 3.9$ or $\beta = 3.8, 3.9$ and 4.05 were also reported. Had we applied instead of eq. (4.7) the other results reported in [38] in order to convert our best-fit parameters into physical units, we would obtain the results of tab. 5. Thus, we can roughly estimate how our final result in eq. (4.8) is systematically affected by the conversion to physical units and consider the central value of $\Lambda_{\overline{\text{MS}}}$ roughly to range from 313 to 335 MeV and that of the gluon condensate from 3.8 to 4.3 GeV^2 . Furthermore, in order to make easier any further comparison (avoiding also the ambiguities related to the conversion to physical units), we collect in tab. 6 the ratios of $\Lambda_{\overline{\text{MS}}}$ and some momentum-dimension physical quantities also obtained in ref. [38]. In particular, if we compare our $N_f = 2$ estimate for $\Lambda_{\overline{\text{MS}}}$, converted to physical units, in eq. (4.8) and the same obtained by applying the Schrödinger functional method in ref. [3], $\Lambda_{\overline{\text{MS}}} = 245(16)(16) \text{ MeV}$, they clearly differ. Nevertheless, had we compared their estimate of $r_0 \Lambda_{\overline{\text{MS}}} = 0.62(4)$ with ours in tab. 6, $r_0 \Lambda_{\overline{\text{MS}}} = 0.72(5)$, we would conclude that they almost agree with each other within their statistical error intervals. Thus, this indicates that the main source of discrepancy for these two results comes from setting the physical scale.

On the other hand, for the purpose of illustrating the effects derived from the dynamical quark mass on the determination of $\Lambda_{\overline{\text{MS}}}$, we can analyze instead of the μ_q -extrapolated data for the coupling (plotted in fig. 4) the ones obtained from the the lattices at $\beta = 4.2$ with $a\mu_q = 0.0065$, $\beta = 4.05$ with $a\mu_q = 0.008$ and $\beta = 3.9$ with $a\mu_q = 0.010$. In view of the results of the lattice spacings ratios in tab. 2 and eq. (4.7), these assumed to be independent of the quark mass, and after the appropriate renormalization,

$$\mu_R = \frac{\mu_q}{Z_P(q_0)} ,\quad (4.9)$$

β 's in fits	$a(3.9)$ (fm)	$\Lambda_{\overline{\text{MS}}}$ (MeV)	$g^2\langle A^2 \rangle$ (GeV ²)
3.9, 4.05, 4.2	0.0801(14)	330(23)	4.2(1.5)
3.9, 4.05	0.0790(26)	335(28)	4.3(1.7)
3.8, 3.9, 4.05	0.0847(15)	313(22)	3.8(1.4)

Table 5: Best-fit parameters for $\Lambda_{\overline{\text{MS}}}$ and the gluon condensate (for which $a(3.9)q_0 = 4.5$ is chosen) by applying the different lattice spacings for $a(3.9)$ obtained in ref. [38] after combined fits including simulations with the different β 's indicated in the first column.

	f_π	f_0	$1/r_0$	$m_{u,d}$
$\Lambda_{\overline{\text{MS}}}$	2.52(18)	2.71(19)	0.72(5)	92(9)

Table 6: dimensionless ratios of $\Lambda_{\overline{\text{MS}}}$ and some momentum dimension quantities taken from ref. [38], where the gauge configurations analyzed in this paper were also exploited. Each number in the table is obtained by dividing the quantity indicated in the row label ($\Lambda_{\overline{\text{MS}}}$) over the one indicated in the column label.

where we apply the $\overline{\text{MS}}$ renormalization constant, Z_P , at the renormalization scale $q_0 = 2$ GeV given in ref. [38], three very similar quark masses will be obtained for the three simulations (see tab. 7). Then, by implementing the ‘‘plateau method’’ with the OPE formula in eq. (2.21), but applying eq. (4.7) to convert into physical units, one will be left with an estimate of $\Lambda_{\overline{\text{MS}}}$ at a renormalized quark mass of the order of $\mu_R \simeq 50$ MeV (see fig. 6). The result of this analysis is:

$$\Lambda_{\overline{\text{MS}}} = 294 \pm 10 \text{ MeV} , \quad (4.10)$$

that appears to indicate a trend that should be kept in mind to compare with previous (or future) unquenched estimates of $\Lambda_{\overline{\text{MS}}}$: the larger is the quark mass, the lower is the estimate of $\Lambda_{\overline{\text{MS}}}$. For instance, in ref. [15], $\Lambda_{\overline{\text{MS}}} = 264$ MeV was reported as the result of a preliminary analysis of the three-gluon coupling from lattice simulations with two flavours of Wilson dynamical quarks and with a renormalized sea-quark mass roughly ranging from 100 to 400 MeV. Both this preliminary results and that of eq. (4.10) seem to be in the right ballpark. So more if one considers the uncertainty derived from the physical lattice calibration previously discussed (see tab. 5) and which makes the central value of $\Lambda_{\overline{\text{MS}}}$ to range from 278 to 298 MeV.

This trend for the behaviour of the estimate for $\Lambda_{\overline{\text{MS}}}$ from the lattice, in particular from the lattice strong coupling in Taylor scheme, is corroborated by the results obtained from the analysis of quenched lattice simulations in ref. [18] (where $\Lambda_{\overline{\text{MS}}} = 224$ MeV). This can be clearly seen in the plots of fig. 6, where the OPE formulae with the values of $\Lambda_{\overline{\text{MS}}}$ and the gluon condensate obtained by fits of results from lattices at $\mu_R = 0$, $\mu_R \sim 50$ in this paper and by a fit of results from quenched lattices in ref. [18] appear displayed. It should be noted that the quenching approximation can be understood as equivalent to consider infinite dynamical quark masses. It may be also worth to remember that, in the three cases, the OPE formulae fit pretty well to the lattice results for the

β	$a\mu_q$	μ_R (MeV)
4.2	0.0065	53.4
4.05	0.008	54.9
3.9	0.010	52.8

Table 7: Quark masses for the three simulations which we re-analyze the results from in order to get an indication of the quark mass effect.

Taylor coupling from momenta roughly ranging from 3 to 6 GeV.

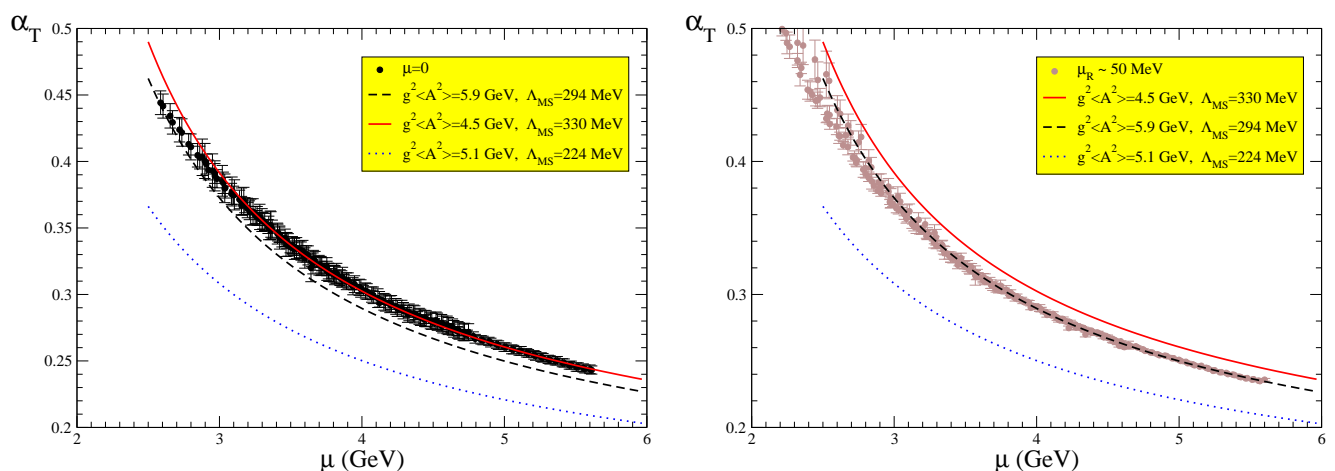


Figure 6: The Taylor coupling after the chiral extrapolation plotted in fig. 5, but now in terms of the momentum in physical units (left), and the same Taylor coupling computed for the three lattice data sets of tab. 7, without chiral extrapolation, also in terms of the momentum in physical units (right). The OPE formula with the best-fit parameters obtained for extrapolated lattice data at $\mu_R = 0$ (solid red line), for the lattice data at $\mu_R \sim 50$ MeV (black dashed line) and for the quenched ($\mu_q \rightarrow \infty$) lattice data in ref. [18] (blue dotted line) are displayed in both plots for the sake of comparison.

5 Discussions and conclusions

We analyzed gauge configurations with twisted $N_f = 2$ dynamical quarks at the *maximal twist* produced by the ETM collaboration for lattices at several β 's (3.9, 4.05, 4.2), and with several different bare twisted masses, and computed the strong coupling constant renormalized in the so-called Taylor scheme. The main advantage of this scheme being not to require any three-point Green function computation, statistical fluctuations became under enough control to permit a very

elaborate treatment of the lattice artefacts and a precise estimate of the couplings at the infinite cut-off limit. The coupling estimates for lattices at different β 's were seen to match pretty well, as should happen if the cut-off limit is properly taken, when plotted in terms of the renormalization momenta converted to the same units by applying the appropriate lattice spacings ratios. These ratios could be either taken from independent computations or obtained by requiring the best matching with pretty compatible results. Indeed, to require the best matching for the strong coupling computed in terms of the momentum for lattices at different β 's was proposed as an alternative method to determine the lattice spacings ratios in ref. [18] and shown here to work pretty well.

Thus, once we are left with the estimates of the coupling constant extrapolated at vanishing dynamical mass μ_q , for every value of the renormalization momentum, μ , they were converted via a fit with a four loops formula into the value of $\Lambda_{\overline{\text{MS}}}$. As also noticed for the analysis of lattice results with $N_f = 0$, the values of $\Lambda_{\overline{\text{MS}}}$ so obtained for every value of μ resulted not to be independent on μ over a momentum window roughly ranging from 2 to 6 GeV. This implies a non-negligible impact of non-perturbative contributions which we accounted for by a Wilson OPE expansion assumed to be dominated by the condensate of the dimension two operator: A^2 . Thus, after including the gluon condensate contribution we recovered a “plateau” for the fitted values of $\Lambda_{\overline{\text{MS}}}$ in terms of the renormalization momentum and estimated the condensate. After discussing the several main sources of systematic uncertainties, specially the higher order contributions in both perturbative and OPE expansions, we converted our fitted parameters into physical units by applying [38]: $a(3.9) = 0.0801(14)$ fm. Thus we obtain $330(23)(22)_{-33}$ MeVs for $\Lambda_{\overline{\text{MS}}}$ and $4.2(1.5)(0.7)$ GeV² for the gluon condensate. As was proven in the quenched case [18], a positive dimension two gluon condensate is unequivocally needed to account for the momentum behaviour of the strong coupling computed from the lattice. Whether condensates of higher order operators have to be included or not in the Wilson expansion is a different matter that cannot be properly addressed with our current data. Indeed, a negative contribution of the order $1/p^4$ can borrow something from the $1/p^2$ gluon condensate, both OPE formulae with and without such a contribution remaining almost totally indistinguishable within our fit momentum window. Then, since the fits including $1/p^4$ contributions become unstable and very noisy, we do not take them into account. A possible way-out could be to perform a cross-check by analyzing the running behaviour of the renormalization constant of other operators. In particular for the quenched case, apart from gluon and ghost operators, the vector part of the quark propagator is studied in ref. [39] and the fitted gluon condensate is found to be compatible with the one obtained from the ghost-gluon vertex [18]. A program to study systematically the non-perturbative OPE contributions to the renormalization constant of quark operators is in progress [40].

Furthermore, we also paid attention to the effect of the dynamical quark masses. As we performed an extrapolation to zero bare twisted mass for the lattice estimates of the strong coupling constant, the $\Lambda_{\overline{\text{MS}}}$ result corresponds to a world with $N_f = 2$ chiral quarks. Nevertheless, for the sake of comparison, we applied the same analysis procedure to three sets of lattice configurations corresponding to practically the same renormalized dynamical quark mass (roughly 50 MeVs),

with no mass extrapolation, and estimated a lighter value of $\Lambda_{\overline{\text{MS}}} = 294(10)$ MeV (the central value can also range from 278 to 298 MeV, depending on which value we use for the lattice spacing in physical units). This is compatible with previous preliminary results ⁸ [15, 16]. We may recall here that the quenched results [18] for $\Lambda_{\overline{\text{MS}}}$ are still lower, ranging mainly around 230 MeV. Since quenching can be understood as the situation with infinite dynamical masses, one may infer a general trend that $\Lambda_{\overline{\text{MS}}}$ increases when the quark mass decreases, with a finite value both at infinite and vanishing quark mass.

As a matter of fact, most of the results for $\Lambda_{\overline{\text{MS}}}$ obtained with Wilson fermions (around 260-270 MeV; see for instance [5] and references therein) lie below our zero-mass result, but also below the phenomenological value which could be obtained, after the appropriated conversion, from the experimental world average, $\alpha(M_Z) = 0.01184(7)$ [41]. The standard procedure to convert $\Lambda_{\overline{\text{MS}}}^{N_f}$ to $\alpha_{\overline{\text{MS}}}$ at a given scale, typically the mass of Z boson, implies the RGE four-loop evolution of the coupling and the three-loop matching at the quark thresholds. Provided that the $\overline{\text{MS}}$ running mass of the charm quark is 1.5 GeV, the conversion from $\Lambda_{\overline{\text{MS}}}^{N_f=3}$ to $\Lambda_{\overline{\text{MS}}}^{N_f=4}$ implies to evolve $\alpha_{\overline{\text{MS}}}$ over an energy range where perturbation theory could fail; but the conversion from $\Lambda_{\overline{\text{MS}}}^{N_f=2}$ to $\Lambda_{\overline{\text{MS}}}^{N_f=3}$ is however out of the scope of the above-described standard conversion procedure. This is why, at present, we prefer not to compare with phenomenological results. This task is to be properly accomplished when $N_f = 2 + 1 + 1$ and $N_f = 4$ lattice simulations will be available. Nevertheless, our current results for $\Lambda_{\overline{\text{MS}}}$ with two light quarks flavours, after chiral extrapolation, seems to point that systematic effects due to the dynamical quark masses could explain the discrepancy between the lattice estimates for the strong coupling with Wilson fermions and its experimental determination.

Acknowledgements

We are particularly indebted to A. Le Yaouanc, J. P. Leroy and J. Micheli for participating in many fruitful discussions at the preliminar stages of this work. We also thank the IN2P3 Computing Center (Lyon) and the apeNEXT computing laboratory (Rome) where part of our simulations have been done. J. R-Q is indebted to the Spanish MICINN for the support by the research project FPA2009-10773 and to “Junta de Andalucía” by P07FQM02962.

⁸The authors of ref. [16] also exploit strong coupling computed on the lattice and renormalized in Taylor scheme, although they presented this scheme as a combination of MOM prescription for the propagators and the $\overline{\text{MS}}$ for the ghost-gluon vertex.

A Appendix: The Wilson coefficients at the four-loops order

The purpose of this appendix is to exploit the four-loops results in ref. [20] to derive the Wilson coefficients with the appropriate renormalization prescription and modify properly eq. (2.21). Following [13, 18] the equations (2.16) for ghost and gluon propagators can be rewritten after renormalization as

$$\begin{aligned} G_R(q^2, \mu^2) &= c_0 \left(\frac{q^2}{\mu^2}, \alpha(\mu^2) \right) + c_2 \left(\frac{q^2}{\mu^2}, \alpha(\mu^2) \right) \frac{\langle A_R^2 \rangle_\mu}{4(N_c^2 - 1)q^2}, \\ F_R(q^2, \mu^2) &= \tilde{c}_0 \left(\frac{q^2}{\mu^2}, \alpha(\mu^2) \right) + \tilde{c}_2 \left(\frac{q^2}{\mu^2}, \alpha(\mu^2) \right) \frac{\langle A_R^2 \rangle_\mu}{4(N_c^2 - 1)q^2}. \end{aligned} \quad (\text{A.1})$$

With the help of the appropriate renormalization constants, one can also write eq. (A.1) in terms of bare quantities:

$$\begin{aligned} G(q^2, \Lambda^2) &= Z_3(\mu^2, \Lambda^2) c_0 \left(\frac{q^2}{\mu^2}, \alpha(\mu^2) \right) \\ &+ Z_3(\mu^2, \Lambda^2) Z_{A^2}^{-1}(\mu^2, \Lambda^2) c_2 \left(\frac{q^2}{\mu^2}, \alpha(\mu^2) \right) \frac{\langle A^2 \rangle}{4(N_c^2 - 1)q^2}, \end{aligned} \quad (\text{A.2})$$

where $A_R^2 = Z_{A^2}^{-1} A^2$. A totally analogous equation for the ghost dressing function $F(q^2, \Lambda^2)$, with \tilde{c}_i and \tilde{Z}_3 in place of c_i and Z_3 . Now, as the μ -dependence of both l.h.s. and r.h.s. of eq. (A.2) should match each other for any q , one can take the logarithmic derivative with respect to μ and infinite cut-off limit, term by term, on r.h.s. and obtains:

$$\begin{aligned} \gamma(\alpha(\mu^2)) + \left\{ \frac{\partial}{\partial \log \mu^2} + \beta(\alpha(\mu^2)) \frac{\partial}{\partial \alpha} \right\} \ln c_0 \left(\frac{q^2}{\mu^2}, \alpha(\mu^2) \right) &= 0 \\ -\gamma_{A^2}(\alpha(\mu^2)) + \gamma(\alpha(\mu^2)) + \left\{ \frac{\partial}{\partial \log \mu^2} + \beta(\alpha(\mu^2)) \frac{\partial}{\partial \alpha} \right\} \ln c_2 \left(\frac{q^2}{\mu^2}, \alpha(\mu^2) \right) &= 0, \end{aligned} \quad (\text{A.3})$$

where $\gamma(\alpha(\mu^2))$ is the gluon propagator anomalous dimension and $\gamma_{A^2}(\alpha(\mu^2))$ is the anomalous dimension for the local operator A^2 defined in eq. (2.20) and that was obtained at four-loop in ref. [28]. Both eqs. (A.3) can be finally combined to give:

$$\left\{ -\gamma_{A^2}(\alpha(\mu^2)) + \frac{\partial}{\partial \log \mu^2} + \beta(\alpha(\mu^2)) \frac{\partial}{\partial \alpha} \right\} \frac{c_2 \left(\frac{q^2}{\mu^2}, \alpha(\mu^2) \right)}{c_0 \left(\frac{q^2}{\mu^2}, \alpha(\mu^2) \right)} = 0, \quad (\text{A.4})$$

and we can proceed in the same way for the ghost dressing function and derive analogous equations for the Wilson coefficients, \tilde{c}_i , that differ from those for c_i only because $\tilde{\gamma}(\alpha(\mu^2))$ takes the place of

$\gamma(\alpha(\mu^2))$. Thus, the combination \tilde{c}_2/\tilde{c}_0 obeys exactly the same eq. (A.4), above derived for c_2/c_0 , that can be solved by applying the following ansatz,

$$\frac{c_2\left(\frac{q^2}{\mu^2}, \alpha(\mu^2)\right)}{c_0\left(\frac{q^2}{\mu^2}, \alpha(\mu^2)\right)} = c_2(1, \alpha(q^2)) \left(\frac{\alpha(\mu^2)}{\alpha(q^2)}\right)^a \left(\frac{1 + \sum_i r_i \alpha^i(\mu^2)}{1 + \sum_i r_i \alpha^i(q^2)}\right), \quad (\text{A.5})$$

where we use that the leading Wilson coefficient is to be renormalized in the MOM renormalization prescription such that $c_0(1, \alpha(\mu^2)) = 1$ and where the exponent a and the coefficients r_i 's are required to satisfy eq. (A.4). Concerning the boundary condition for c_2 , the prescription applied for the renormalization of the local operator A^2 to obtain its four-loops anomalous dimension, γ_{A^2} , in [28] is the standard $\overline{\text{MS}}$ and, with this prescription, c_2 is computed at the four-loop order in ref. [20] (see the eq. (7) of that paper). We only need to take $q^2 = \mu^2$ in the expression given in ref. [20] and have thus $c_2(1, \alpha(\mu^2))$. Then, one obtains at the four-loop order:

$$\begin{aligned} \frac{c_2\left(\frac{q^2}{\mu^2}, \alpha(\mu^2)\right)}{c_0\left(\frac{q^2}{\mu^2}, \alpha(\mu^2)\right)} &= 3\bar{g}^2(\mu^2) \left(\frac{\bar{\alpha}(q^2)}{\bar{\alpha}(\mu^2)}\right)^{\frac{27}{116}} (1 + 2.1930 \bar{\alpha}(q^2) + 6.1460 \bar{\alpha}^2(q^2) + 20.5477 \bar{\alpha}^3(q^2)) \\ &\times (1 + 0.0208 \bar{\alpha}(\mu^2) + 0.0095 \bar{\alpha}^2(\mu^2) + 0.0164 \bar{\alpha}^3(\mu^2)), \end{aligned} \quad (\text{A.6})$$

where the loop expansion is given in terms of the $\overline{\text{MS}}$ coupling, $\bar{\alpha}$.

Concerning \tilde{c}_2/\tilde{c}_0 , as it obeys the same differential equation eq. (A.4), the solution differ from the one for the gluon propagator only because of the boundary condition which will be now obtained from eq. (9) of ref. [20]. Thus, one obtains at the four-loop order:

$$\begin{aligned} \frac{\tilde{c}_2\left(\frac{q^2}{\mu^2}, \alpha(\mu^2)\right)}{\tilde{c}_0\left(\frac{q^2}{\mu^2}, \alpha(\mu^2)\right)} &= 3\bar{g}^2(\mu^2) \left(\frac{\bar{\alpha}(q^2)}{\bar{\alpha}(\mu^2)}\right)^{\frac{27}{116}} (1 + 1.1728 \bar{\alpha}(q^2) + 2.7098 \bar{\alpha}^2(q^2) + 8.4690 \bar{\alpha}^3(q^2)) \\ &\times (1 + 0.0208 \bar{\alpha}(\mu^2) + 0.0095 \bar{\alpha}^2(\mu^2) + 0.0164 \bar{\alpha}^3(\mu^2)). \end{aligned} \quad (\text{A.7})$$

Thus, we can combine both eqs. (A.6,A.7), as done in eq. (2.19), to obtain:

$$\begin{aligned} \alpha_T(q^2) &= \alpha_T^{\text{pert}}(q^2) \left(1 + \frac{9}{q^2} \frac{\bar{g}^2(\mu^2) \langle A^2 \rangle_{R, \mu^2}}{4(N_C^2 - 1)} \left(\frac{\bar{\alpha}(q^2)}{\bar{\alpha}(\mu^2)}\right)^{\frac{27}{116}} \right. \\ &\times (1 + 1.5129 \bar{\alpha}(q^2) + 3.8552 \bar{\alpha}^2(q^2) + 12.4952 \bar{\alpha}^3(q^2)) \\ &\times \left. (1 + 0.0208 \bar{\alpha}(\mu^2) + 0.0095 \bar{\alpha}^2(\mu^2) + 0.0164 \bar{\alpha}^3(\mu^2)) \right). \end{aligned} \quad (\text{A.8})$$

Finally, provided that the purely perturbative part of the OPE formula in eq. (A.8) is the coupling renormalized in the T-scheme, it seems more appropriate to expand in terms of α_T instead of $\bar{\alpha}$.

Then, one can apply eqs. (2.9,2.10) for the conversion and obtain:

$$\begin{aligned}
\alpha_T(q^2) = \alpha_T^{\text{pert}}(q^2) & \left(1 + \frac{9}{q^2} \frac{g_T^2(\mu^2) \langle A^2 \rangle_{R,\mu^2}}{4(N_C^2 - 1)} \left(\frac{\alpha_T(q^2)}{\alpha_T(\mu^2)} \right)^{\frac{27}{116}} \right. \\
& \times (1 + 1.2932 \alpha_T(q^2) + 1.9363 \alpha_T^2(q^2) + 3.8296 \alpha_T^3(q^2)) \\
& \left. \times (1 - 0.7033 \alpha_T(\mu^2) - 0.3652 \alpha_T^2(\mu^2) + 0.0051 \alpha_T^3(\mu^2)) \right) .(A.9)
\end{aligned}$$

References

- [1] M. Luscher, R. Sommer, P. Weisz and U. Wolff, Nucl. Phys. B **413** (1994) 481; S. Capitani, M. Luscher, R. Sommer and H. Wittig [ALPHA Collaboration], Nucl. Phys. B **544** (1999) 669 [arXiv:hep-lat/9810063].
- [2] G. M. de Divitiis, R. Frezzotti, M. Guagnelli and R. Petronzio, Nucl. Phys. B **433** (1995) 390 [arXiv:hep-lat/9407028].
- [3] M. Della Morte, R. Frezzotti, J. Heitger, J. Rolf, R. Sommer and U. Wolff [ALPHA Collaboration], Nucl. Phys. B **713** (2005) 378 [arXiv:hep-lat/0411025].
- [4] S. Aoki *et al.* [PACS-CS Collaboration], JHEP **0910** (2009) 053 [arXiv:0906.3906 [hep-lat]].
- [5] M. Gockeler, R. Horsley, A. C. Irving, D. Pleiter, P. E. L. Rakow, G. Schierholz and H. Stuben, Phys. Rev. D **73** (2006) 014513 [arXiv:hep-ph/0502212].
- [6] K. Maltman, D. Leinweber, P. Moran and A. Sternbeck, Phys. Rev. D **78** (2008) 114504 [arXiv:0807.2020 [hep-lat]].
- [7] C. T. H. Davies, K. Hornbostel, I. D. Kendall, G. P. Lepage, C. McNeile, J. Shigemitsu and H. Trotter [HPQCD Collaboration], Phys. Rev. D **78** (2008) 114507 [arXiv:0807.1687 [hep-lat]].
- [8] Q. Mason *et al.* [HPQCD Collaboration and UKQCD Collaboration], Phys. Rev. Lett. **95** (2005) 052002 [arXiv:hep-lat/0503005].
- [9] B. Alles, D. Henty, H. Panagopoulos, C. Parrinello, C. Pittori and D. G. Richards, Nucl. Phys. B **502** (1997) 325 [arXiv:hep-lat/9605033].
- [10] P. Boucaud, J. P. Leroy, J. Micheli, O. Pene and C. Roiesnel, JHEP **9810** (1998) 017 [arXiv:hep-ph/9810322].
- [11] P. Boucaud *et al.*, JHEP **0004** (2000) 006 [arXiv:hep-ph/0003020].
- [12] Ph. Boucaud, A. Le Yaouanc, J.P. Leroy, J. Micheli, O. Pène, J. Rodriguez-Quintero, Phys. Lett. B **493** (2000) 315;
- [13] Ph. Boucaud, A. Le Yaouanc, J.P. Leroy, J. Micheli, O. Pène, J. Rodriguez-Quintero, Phys. Rev. D **63** (2001) 114003; F. De Soto and J. Rodriguez-Quintero, Phys. Rev. D **64** (2001) 114003 .
- [14] P. Boucaud *et al.*, Phys. Rev. D **66** (2002) 034504; JHEP **0304** (2003) 005; Phys. Rev. D **70** (2004) 114503.
- [15] P. Boucaud, J. P. Leroy, H. Moutarde, J. Micheli, O. Pene, J. Rodriguez-Quintero and C. Roiesnel, JHEP **0201** (2002) 046 [arXiv:hep-ph/0107278].

- [16] A. Sternbeck, K. Maltman, L. von Smekal, A. G. Williams, E. M. Ilgenfritz and M. Muller-Preussker, PoS **LAT2007** (2007) 256 [arXiv:0710.2965 [hep-lat]]; A. Sternbeck, E. M. Ilgenfritz, K. Maltman, M. Mueller-Preussker, L. von Smekal and A. G. Williams, PoS **LAT2009** (2009) 210 [arXiv:1003.1585 [hep-lat]].
- [17] F. V. Gubarev and V. I. Zakharov, Phys. Lett. B **501** (2001) 28 [arXiv:hep-ph/0010096]; D. Dudal, H. Verschelde and S. P. Sorella, Phys. Lett. B **555** (2003) 126 ; K. I. Kondo, Phys. Lett. B **572** (2003) 210 ; [arXiv:hep-th/0306195]. Phys. Lett. B **514** (2001) 335 [arXiv:hep-th/0105299]; E. Megias, E. Ruiz Arriola and L. L. Salcedo, Phys. Rev. D **75** (2007) 105019 [arXiv:hep-ph/0702055].
- [18] Ph. Boucaud, F. De Soto, J. P. Leroy, A. Le Yaouanc, J. Micheli, O. Pene and J. Rodriguez-Quintero, Phys. Rev. D **79** (2009) 014508 [arXiv:0811.2059 [hep-ph]].
- [19] Ph. Boucaud *et al.* [ETM collaboration], Comput. Phys. Commun. **179** (2008) 695 [arXiv:0803.0224 [hep-lat]].
- [20] K. G. Chetyrkin and A. Maier, arXiv:0911.0594 [hep-ph].
- [21] J. C. Taylor, Nuclear Physics B33 (1971) 436
- [22] K. G. Chetyrkin and A. Retey, [arXiv:hep-ph/0007088].
- [23] K. G. Chetyrkin, Nucl. Phys. B **710** (2005) 499 [arXiv:hep-ph/0405193];
- [24] T. van Ritbergen, J. A. M. Vermaseren and S. A. Larin, Phys. Lett. B **400** (1997) 379 [arXiv:hep-ph/9701390]; M. Czakon, Nucl. Phys. B **710** (2005) 485 [arXiv:hep-ph/0411261].
- [25] R. Wilson, Phys. Rev. **179** (1969) 1499.
- [26] Ph. Boucaud *et al.*, JHEP **0601** (2006) 037 [arXiv:hep-lat/0507005]; Ph. Boucaud, A. Le Yaouanc, J.P. Leroy, J. Micheli, O. Pène, J. Rodriguez-Quintero, Phys. Rev. **D63** (2001) 114003
- [27] M.A. Shifman, A.I. Vainshtein, V.I. Zakharov, Nucl. Phys. **B147** (1979) 385,447,519; M.A. Shifman, A.I. Vainshtein, M.B. Voloshin, V.I. Zakharov, Phys. Lett. **B77** (1978) 80;
- [28] J. A. Gracey, Phys. Lett. B **552** (2003) 101 [arXiv:hep-th/0211144].
- [29] P. Weisz, Nucl. Phys. B **212** (1983) 1.
- [30] R. Frezzotti, P. A. Grassi, S. Sint and P. Weisz [Alpha collaboration], JHEP **0108** (2001) 058 [arXiv:hep-lat/0101001].
- [31] Ph. Boucaud *et al.* [ETM Collaboration], Phys. Lett. B **650** (2007) 304 [arXiv:hep-lat/0701012].
- [32] C. Urbach [ETM Coll.], PoS **LAT2007** (2007) 022 [0710.1517 [hep-lat]].
- [33] P. Dimopoulos *et al.* [ETM Collaboration], arXiv:0810.2873 [hep-lat].
- [34] R. Frezzotti and G. C. Rossi, JHEP **0408** (2004) 007 [arXiv:hep-lat/0306014].

- [35] Ph. Boucaud *et al.*, Phys. Rev. D **72** (2005) 114503 [arXiv:hep-lat/0506031].
- [36] D. Becirevic, P. Boucaud, J. P. Leroy, J. Micheli, O. Pene, J. Rodriguez-Quintero and C. Roiesnel, Phys. Rev. D **60** (1999) 094509 [arXiv:hep-ph/9903364].
- [37] F. de Soto and C. Roiesnel, JHEP **0709** (2007) 007 [arXiv:0705.3523 [hep-lat]].
- [38] R. Baron *et al.* [ETM Collaboration], arXiv:0911.5061 [hep-lat].
- [39] Ph. Boucaud *et al.*, Phys. Rev. D **74** (2006) 034505 [arXiv:hep-lat/0504017].
- [40] Ph. Boucaud *et al.* [ETM Collaboration], *In progress*.
- [41] C. Amsler *et al.* [Particle Data Group], Phys. Lett. B **667** (2008) 1.